Bone Remodeling Under Tooth Loading

Kangning Su, Li Yuan and Jing Du

Abstract The stability and success rate of orthopedic and dental implants are affected by their surrounding bone quality. Bone adapts to mechanical loads through remodeling activities to achieve new equilibrium in strain/stress state. The object of this study is to develop a numerical algorithm to simulate bone remodeling activities under mechanical loading. Finite element method is used to calculate the strain/stress distribution in the alveolar bone under tooth loading. The bone density remains unchanged near the equilibrium point of the mechanical stimulus; under greater or smaller mechanical stimulus, it increases or decreases. Iterations are performed to simulate the evolution of bone density. Effects of model geometry and adjacent teeth are studied. Effects of various applied loads and boundary conditions are compared. Simulation results are validated using computed tomography (CT) data of human mandibles. The implications of the results on patient-specific treatment and the insights for clinical techniques are also discussed.

Keywords Bone remodeling · Finite element · Dentistry

Introduction

Teeth are attached to jaw bone through the periodontal ligament (PDL). Bone is a living tissue. It has the ability to adapt to the change of mechanical stimulus [1]. Generally, the increase and decrease of mechanical stimulus promote bone

K. Su · J. Du (✉)
Department of Mechanical and Nuclear Engineering,
Pennsylvania State University, State College, USA
e-mail: jingdu@psu.edu

K. Su
e-mail: conysu666@gmail.com

L. Yuan
Shenzhen People's Hospital, 2nd Clinical Medical College
of Jinan University, Guangzhou, China

The Minerals, Metals & Materials Society, *TMS 2017 146th Annual Meeting & Exhibition Supplemental Proceedings*, The Minerals, Metals & Materials Series,
DOI 10.1007/978-3-319-51493-2_31

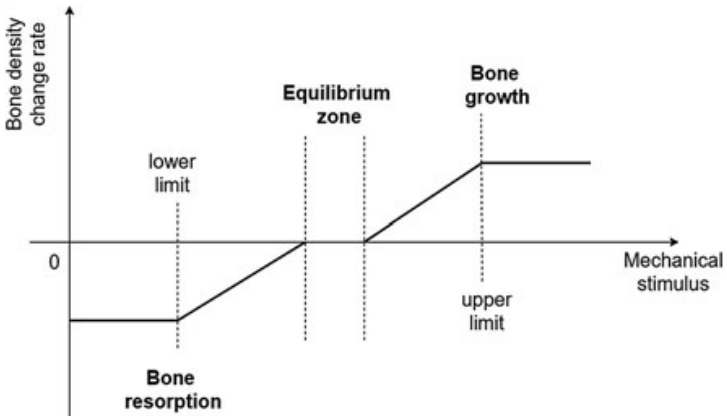

Fig. 1 Bone density change rate against mechanical stimulus

formation and resorption activities, respectively. The resorption and formation processes of bone are called bone remodeling. It has been studied using various animal experiments [2, 3] and numerical simulations, such as finite element method [4, 5].

In numerical simulations, bone remodeling is usually represented by the change of bone density. A commonly used rule [6] for bone density change is presented in Fig. 1. The mechanical stimulus can be mechanical strain [7], daily stress [8], strain energy density [9] or micro-damage [7]. Inside the equilibrium zone, the desired value of mechanical stimulus retains the bone density. When the applied mechanical stimulus is less than the desired value, bone density decreases due to bone disuse. In contrast, when the applied mechanical stimulus is greater than equilibrium, bone overuse causes the increase of bone density.

In the simplified model in Fig. 1, the rate of density change is linearly proportional to the difference between the applied mechanical stimulus and the equilibrium zone. When the mechanical stimulus is beyond the upper or lower thresholds, the bone density changes at a constant rate. In other works [5], parabolic relation between density change rate and mechanical stimulus were used. In such cases, when the applied mechanical stimulus was much greater than equilibrium, it caused overload bone resorption.

In this study, the trabecular bone density is assumed to be uniform initially. Finite element method is used to calculate the strain energy density in teeth and their surrounding tissues under normal chewing and biting forces. The bone density change was calculated using the bone remodeling algorithm. Iterations are carried out to simulate the adaptation of bone density over multiple time steps. Several model geometries and boundary conditions are used to study the effects of adjacent teeth. Computed tomography (CT) data of human mandibles are used to validate the simulation results. The implications of the results on patient-specific treatment and the insights for clinical techniques are also discussed.

Bone Remodeling Simulations

Finite Element Model

The finite element simulations were carried out using the Abaqus FEA software package (Dassault Systemes Simulia Corporation, Providence, RI) to calculate the strain energy density in the tooth-bone structures under normal chewing force. 2-dimensional (2D) models were built to simplify the geometry of natural human teeth in the jaw bone, as shown in Fig. 2. Figure 2a shows lateral incisor and its surrounding soft and hard tissues. Figure 2b shows central and lateral incisors, canine and their surrounding tissues. The dimensions of the mandible bone and the geometry of the lateral incisor were the same in both models. They each consisted of enamel, dentin, pulp, cementum, periodontal ligament (PDL), gingiva, cortical bone and trabecular bone. The geometry and dimensions of the models were based on the average anatomy of natural human teeth [10]. The thickness of cortical bone layer was 2 mm.

4-node linear quadrilateral element was used in the mesh. An identical load was applied on each tooth to simulate the normal chewing and biting force [11]. It consisted of a lateral force of 10 N to the right (mesial direction) and a vertical force of 100 N. The bottom of the model was fixed. Two kinds of boundary conditions were used for the left and right boundaries of the model. In one case, the two sides were constrained to move only in the vertical direction. In the other case, they were set to be free.

The material properties of the teeth and their surrounding tissues used in the simulations are listed in Table 1 [12]. All the materials were assumed to be linear elastic and isotropic.

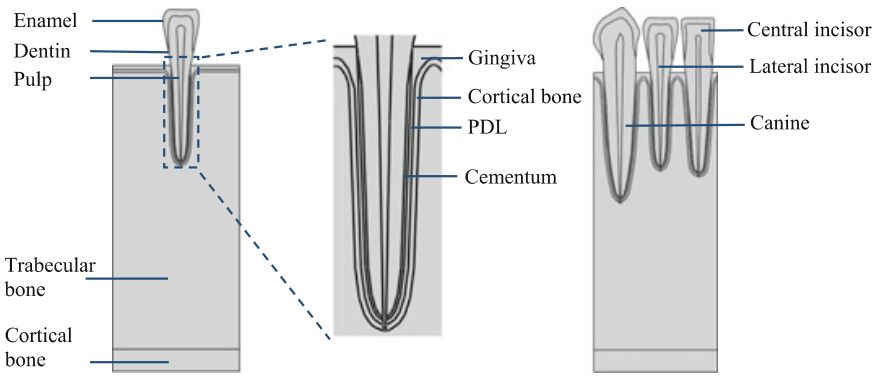

Fig. 2 Finite element model of **a** lateral incisor and **b** central and lateral incisors, canine and their surrounding soft and hard tissues

Table 1 Material properties used in the finite element simulations

Materials	Enamel	Dentin	Pulp	Cementum	Periodontal ligament	Gingiva	Cortical bone	Cancellous bone
Young's modulus (GPa)	79.6	18.6	0.15	13.7	0.2	0.2	13.7	1.5
Poisson's ratio	0.3	0.31	0.49	0.3	0.45	0.45	0.3	0.33

Bone Density and Young's Modulus

Carter and Hayes [13] suggested an empirical relationship between trabecular bone density and its Young's modulus:

$$E = C\rho^3 \tag{1}$$

where E is the Young's modulus in GPa, C is a constant, which in this case is 3740, and ρ is the apparent density in g/cm^3. Equation (1) was used to calculate the bone density in the initial condition and to change the Young's modulus of trabecular bone in the following steps.

Bone Remodeling Algorithm

The flow chart of the bone remodeling algorithm is presented in Fig. 3. The algorithm was implemented using Python scripts to set up and run finite element simulations in Abaqus. The density and Young's modulus in the trabecular bone were assumed to be uniform in the initial conditions. The strain energy density in the tooth-bone structure was calculated using the model presented in "Finite Element Model". The bone density change was calculated using the remodeling rules [14] given by

$$\text{Bone loss at constant rate: } \Delta\rho = -0.05 \cdot B \cdot \Delta t, \text{ if } \frac{U}{\rho} < \Xi_l \tag{2}$$

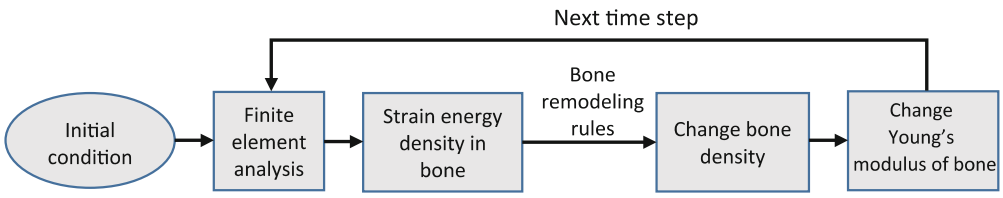

Fig. 3 Flow chart of the bone remodeling algorithm

$$\text{Bone loss: } \Delta\rho = B\left(\frac{U}{\rho} - (1-\delta)\Xi\right)\cdot\Delta t, \text{ if } 0.05\cdot B + (1-\delta)\Xi < \frac{U}{\rho} < (1-\delta)\Xi \tag{3}$$

$$\text{Bone equilibrium: } \Delta\rho = 0, \text{ if} (1-\delta)\Xi < \frac{U}{\rho} < (1+\delta)\Xi \tag{4}$$

$$\text{Bone growth: } \Delta\rho = B\left(\frac{U}{\rho} - (1+\delta)\Xi\right)\cdot\Delta t, \text{ if} (1+\delta)\Xi < \frac{U}{\rho} < 0.05\cdot B + (1+\delta)\Xi \tag{5}$$

$$\text{Bone growth at constant rate: } \Delta\rho = 0.05\cdot B\cdot\ \Delta t, \text{ if } \frac{U}{\rho} > \Xi_u \tag{6}$$

where U is the strain energy density, Ξ is the reference strain energy density per unit bone mass, Ξ_u and Ξ_l are the upper and lower limit of strain energy density shown in Fig. 1. δ is the range factor for the equilibrium zone, B is the remodeling constant, and t is time. In this case, Ξ is 0.0036 J/(g cm^3), δ is 10% and B is 10 (time unit · g/cm^5). A small time increment was used to assure convergence, thus Δt was set to be 0.2 s. In natural teeth, the trabecular bone is less dense than cortical bone. Therefore, ρ is set to be less or equal to 2.0 g/cm^3. Also, it is set to be greater than 0.1 g/cm^3. [15] The Young's modulus of each element was then calculated using Eq. (1).

Results and Discussion

Strain Energy Density and Bone Density

For the 3-tooth model, simulation results at the 5th, 10th, 15th and 25th time steps are presented in Figs. 4 and 5, respectively, for constrained and free boundary conditions. It can be observed that the strain energy density initially concentrated near the apical region of the teeth. As time goes by, strain energy density dissipated into other regions of the structure and resulted in a more uniform distribution. Moreover, the overall strain energy density in trabecular bone reduced over time.

Bone density was set to be uniform in trabecular bone initially. During the bone remodeling processes, bone density gradually changed under load. The bone density increased between tooth roots, where strain energy density was greater. It also increased in the right side of the model (mesial side), towards the direction of the applied load.

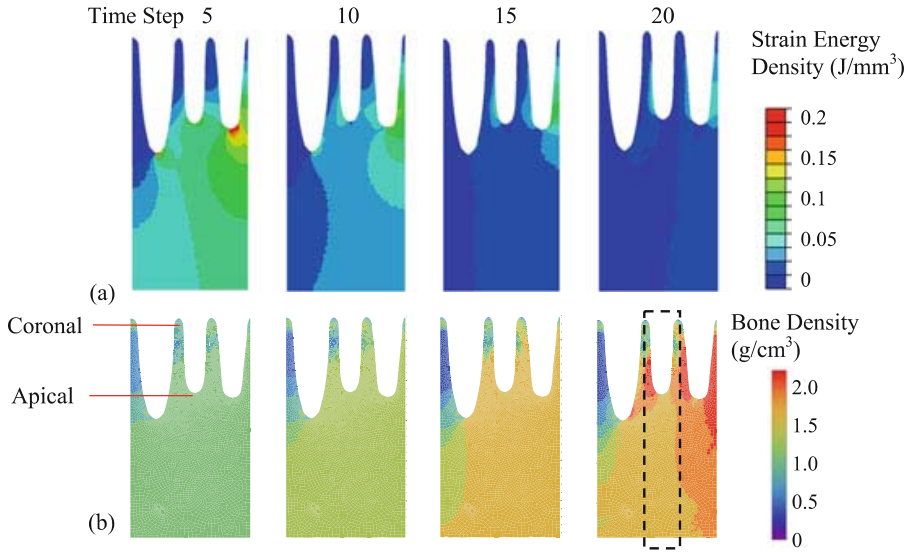

Fig. 4 **a** Strain energy density and **b** bone density in the 3-tooth model with constrained boundary conditions

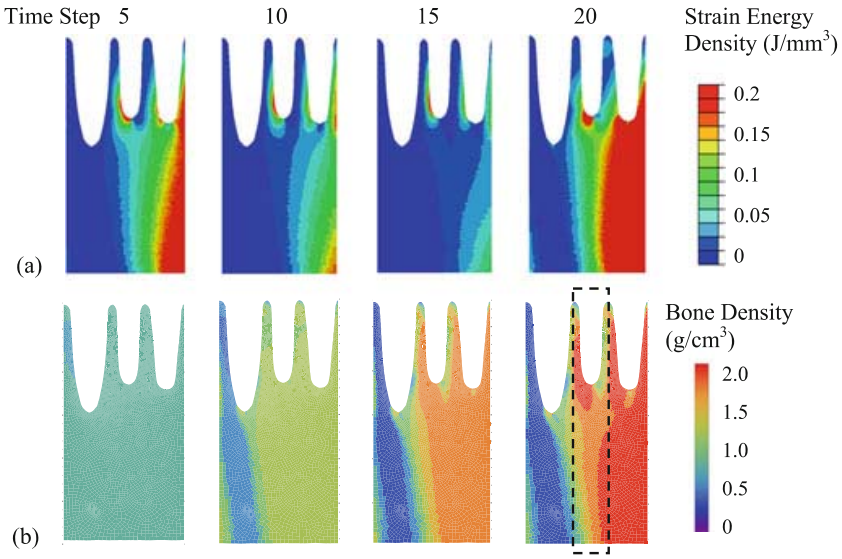

Fig. 5 **a** Strain energy density and **b** bone density in the 3-tooth model with free boundary conditions

Boundary Conditions

The results from models using constrained or free boundary conditions were similar in the vicinity of the lateral incisor. For the two boundary conditions, the bone density intensity increased between lateral incisor and its adjacent teeth during the remodeling process. Generally, the bone density value was lower in the coronal region and higher in the apical region. Below the lateral incisor, the bone density distribution is more uniform when the boundary was constrained (Fig. 4b).

When the boundary was set free, the variation in the bone density below the lateral incisor is more severe (Fig. 5b).

The actual teeth movement is constrained by their adjacent teeth and jaw bone. Therefore, the constrained boundary condition may be a better representation of the actual situation. Furthermore, the boundaries should be set far away from the region of interest. In other words, the results in the middle of the model (near the lateral incisor) are more reliable than those close to the left and right boundaries of the model.

Adjacent Teeth

Figure 6 shows the results obtained from the 1-tooth model with constrained boundary conditions. Strain energy density was higher towards the direction of applied load. The overall variation of the strain energy density decreased during bone remodeling process. It increased below the tooth in the direction of the applied load. The bone density also increased in the similar regions below and to the right of the tooth. In contrast, bone density to the left of the tooth drastically decreased. When adjacent teeth were missing, with fewer constraints, the density variation in the left (distal) and right (mesial) sides of the tooth was more severe.

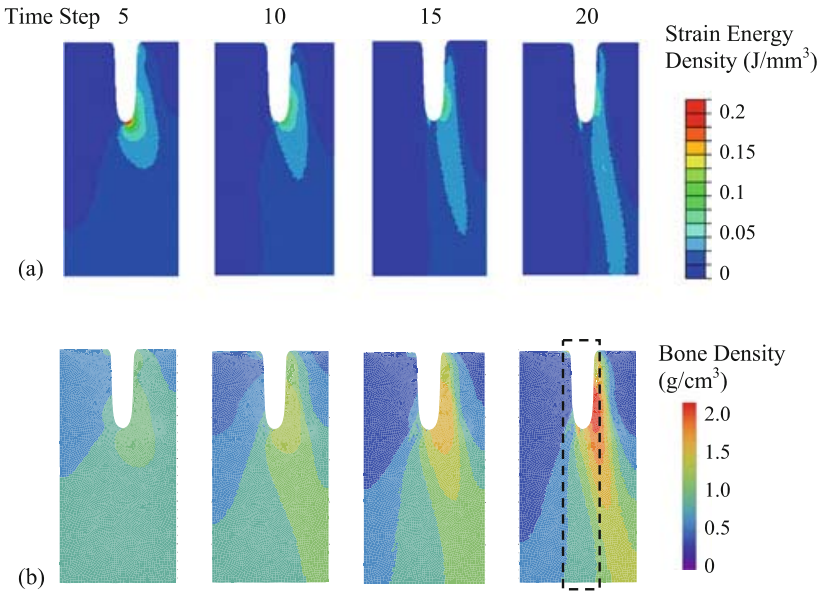

Fig. 6 **a** Strain energy density and **b** bone density in the 1-tooth model with constrained boundary conditions

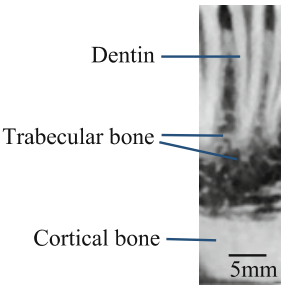

Fig. 7 A slice of dental cone beam computed tomography (CT) images

Computed Tomography (CT) Scans

A virtual slice of the dental computed tomography (CT) images of a human jaw is presented in Fig. 7. The greyscale of the image represents the density of the bone. As shown in Fig. 7, the density of cortical bone is much higher than trabecular bone. The trabecular bone around the lateral incisor is relatively denser than those below the tooth. There is not significant variation in the bone density beneath the tooth. These are in agreement with the bone density distribution obtained from 3-tooth model with constrained boundary conditions.

Implications

The current results suggest that there is a relationship between the applied load and the bone density distribution in jaw bone. Human teeth have the natural tendency to move towards the front and center (mesial drift) [16]. Moreover, jaw bone level decreases rapidly in the first 6 months to 2 years following tooth extraction. [17] Bone remodeling simulations can provide insights to these dental phenomena. However, there is a need to develop more accurate bone remodeling models.

There are several limitations in the current model. For example, the initial bone density was set to be uniform. Also, other stimulus for bone remodeling, such as biochemical signals, were ignored in the model. Further work is also needed to assess the actual geometry of teeth in jaw bone and the anisotropic and viscoelastic mechanical properties of the tissues.

Conclusion

This paper presents the results of the numerical simulations of jaw bone remodeling processes during normal chewing and biting activities. Bone increased at the regions where the mechanical stimulus (strain energy density) was greater, and *vice versa*. The variations in mechanical stimulus in the whole structure reduced over time. The overall level of the mechanical stimulus also reduced. With constrained

boundaries far from the region of interest, results obtained from 3-tooth model were in agreement with the dental CT data. Without constrained boundaries, the results were not comparable to CT data in the regions below the tooth. Without the presence of the adjacent teeth, bone density in the left (distal) side of the tooth decreased drastically in the 1-tooth model.

Acknowledgements This study is supported by the Department of Mechanical and Nuclear Engineering and Institute for Cyber Science (ICS) at the Pennsylvania State University. The authors are grateful to Dr. Reuben Kraft for useful technical discussions.

References

1. J. Wolff, *The Law of Bone Remodeling* (Springer, New York, 1986)
2. L.P. Maia, D.M. Reino, A.B. Novaes, V.A. Muglia, M. Taba, M.F. de Morais Grisi, S.L.S. de Souza, D.B. Palioto, Influence of periodontal biotype on buccal bone remodeling after tooth extraction using the flapless approach with a xenograft: a histomorphometric and fluorescence study in small dogs. Clin. Implant Dent. Relat. Res. **17**, e221–e235 (2015)
3. B.A. Gultekin, P. Gultekin, S. Yalcin, Application of finite element analysis in implant dentistry. Finite Elem. Anal. New Trends Dev. 21–54 (2012)
4. C. Bourauel, D. Vollmer, A. Jäger, Application of bone remodeling theories in the simulation of orthodontic tooth movements. J. Orofac. Orthop. / Fortschritte der Kieferorthopädie **61**(4), 266 (2000)
5. J. Li, H. Li, L. Shi, A.S.L. Fok, C. Ucer, H. Devlin, K. Horner, N. Silikas, A mathematical model for simulating the bone remodeling process under mechanical stimulus. Dent. Mater. **23**(9), 1073–1078 (2007)
6. J. Martínez-Reina, J. Ojeda, J. Mayo, On the use of bone remodelling models to estimate the density distribution of bones. Uniqueness of the solution. PLoS One **11**(2), e0148603 (2016)
7. B.P. McNamara, D. Taylor, P.J. Prendergast, Computer prediction of adaptive bone remodelling around noncemented femoral prostheses: the relationship between damage-based and strain-based algorithms. Med. Eng. Phys. **19**(5), 454–463 (1997)
8. D.J. Adams, A.A. Spirt, T.D. Brown, S.P. Fritton, C.T. Rubin, R.A. Brand, Testing the daily stress stimulus theory of bone adaptation with natural and experimentally controlled strain histories. J. Biomech. **30**(7), 671–678 (1997)
9. A. Mellal, H.W.A. Wiskott, J. Botsis, S.S. Scherrer, U.C. Belser, Stimulating effect of implant loading on surrounding bone. Comparison of three numerical models and validation by in vivo data. Clin. Oral Implants Res. **15**(2), 239–248 (2004)
10. D.L. Bird, D.S. Debbie S, *Modern Dental Assisting* (Elsevier Health Sciences, 2013)
11. T.M.G.J. van Eijden, J.H. Koolstra, P. Brugman, W.A. Weijs, A feedback method to determine the three-dimensional bite-force capabilities of the human masticatory system. J. Dent. Res. **67**(2), 450–454 (1988)
12. M. Su, H. Chang, Y. Chiang, J. Cheng, L.-J. Fuh, C.-Y. Wang, C.-P. Lin, Modeling viscoelastic behavior of periodontal ligament with nonlinear finite element analysis. J. Dent. Sci. **8**(2), 121–128 (2013)
13. D.R. Carter, W.C. Hayes, The compressive behavior of bone as a two-phase porous structure. J. Bone Joint Surg. Am. **59**(7), 954–962 (1977)
14. D. Lin, Q. Li, W. Li, P. Rungsiyakull, M. Swain, Bone resorption induced by dental implants with ceramics crowns **45**, 1–7 (2009)

15. Z. Lian, H. Guan, S. Ivanovski, Y.-C. Loo, N. Johnson, H. Zhang, Finite element simulation of bone remodelling in the human mandible surrounding dental implant. Acta Mech. **217**(3–4), 335–345 (2011)
16. A. Nanci, A.R. Ten Cate, *Ten Cate's Oral Histology: Development, Structure, and Function* (Elsevier, 2013), p. 379
17. D.A. Atwood, Bone loss of edentulous alveolar ridges. J. Periodontol. **50**(4s), 11–21 (1979)